Ocean Sci. Discuss., https://doi.org/10.5194/os-2017-58
Manuscript under review for journal Ocean Sci.
Discussion started: 28 July 2017

Ocean Science
Discussions
Open Access
EGU

Quantifying thermohaline circulations: seawater isotopic compositions and salinity as proxies of the ratio between advection time and evaporation time

Hadar Berman, Nathan Paldor* and Boaz Lazar

The Fredy and Nadine Herrmann Institute of Earth Sciences

The Hebrew University of Jerusalem

*Corresponding author, Email address: nathan.paldor@mail.huji.ac.il

Ocean Sci. Discuss., https://doi.org/10.5194/os-2017-58
Manuscript under review for journal Ocean Sci.
Discussion started: 28 July 2017

Ocean Science
Discussions
Open Access
EGU

23 Abstract

24 Uncertainties in quantitative estimates of the thermohaline circulation in any particular basin
25 are large, partly due to large uncertainties in quantifying excess evaporation over precipitation
26 and surface velocities. A single nondimensional parameter, $\gamma \equiv \frac{q}{h}\frac{x}{u}$ is proposed to
27 characterize the "strength" of the thermohaline circulation by combining the physical
28 parameters of surface velocity (u), evaporation rate (q), mixed layer depth (h) and trajectory
29 length (x). Values of γ can be estimated directly from cross-sections of salinity or seawater
30 isotopic composition ($\delta^{18}O$ and δD). Estimates of γ in the Red Sea and the South-West Indian
31 Ocean are 0.1 and 0.02, respectively, which implies that the thermohaline contribution to the
32 circulation in the former is higher than in the latter. Once the value of γ has been determined
33 in a particular basin, either q or u can be estimated from known values of the remaining
34 parameters. In the studied basins such estimates are consistent with previous studies.

Ocean Sci. Discuss., https://doi.org/10.5194/os-2017-58
Manuscript under review for journal Ocean Sci.
Discussion started: 28 July 2017

1. Introduction

The thermohaline circulation is driven by net evaporation-precipitation from the surface layer, which is compensated for by horizontal advection of (typically) small speeds. This circulation has been used to describe the circulation in various parts of the world ocean including semi-enclosed basins (such as the Red Sea). Due to the small horizontal velocities and excess of evaporation (i.e. evaporation minus precipitation) it is difficult to directly quantify the thermohaline circulation in terms of the mean water speed and/or the water column transport. The aim of this paper is to propose a single non-dimensional parameter that quantifies the advection vs. evaporation (referred later as the "strength") of the thermohaline circulation.

While mean velocities are small and hard to measure (since they do not differ from their instantaneous variability), net evaporation over land has been measured for decades by dish-pan evaporation experiments, in which the level of water in a pan (or shallow lagoon) located on a coast is monitored over several weeks/months. Over sea however, these experiments are not accurate since they cannot generate the microclimate of a large semi-enclosed basin or ocean. For example, values of 3.5 $m \cdot y^{-1}$ (Sofianos et. al, 2002; Vercelli, 1925) and 3.1 $m \cdot y^{-1}$ (Cohen et al., 1977) were found for the Red Sea, both of which turned out to be too high (compared with detailed heat balance calculations, Ben-Sasson et al., 2009).

Net evaporation in the ocean can be estimated only crudely from routine salinity measurements. The reason for this uncertainty is the difficulty in separating the mean salinity difference across the surface layer from temporal (e.g. seasonal) and spatial (i.e. the depth above which the incoming waters flow) differences. This is why salinity based estimates of net evaporation in a particular basin may vary by up to 100% even though the different ways in which salinity has been measured in the last several decades have not yielded drastically different values. For example, in the Red Sea net evaporation rates range between 1.7 $m \cdot y^{-1}$ (Tragou, 1999) and 2.7 $m \cdot y^{-1}$ (Sofianos et. al, 2002; Bogdanova, 1974) even though both

Ocean Sci. Discuss., https://doi.org/10.5194/os-2017-58
Manuscript under review for journal Ocean Sci.
Discussion started: 28 July 2017

studies employed the same salt-conservation methodology i.e. assessing salinity differences between incoming and outgoing waters.

Attempts to estimate the net evaporation from detailed calculations of the various components of the heat balance in semi-enclosed basins (i.e. incoming shortwave radiation, net outgoing longwave radiation, latent heat release and advection of heat to/from the basin) encountered similar discrepancies. In the northern Red Sea, the detailed heat flux calculation by Assaf and Kessler (1976) have yielded a net evaporation rate of 3.6 $m \cdot y^{-1}$ while Ben-Sasson et al. (2009) and Berman et al. (2003) estimated the annual net evaporation rate to be only 1.8 $m \cdot y^{-1}$ (see also, Sofianos, 2002).

An approach of using fractionation of stable isotopes of oxygen and hydrogen has been previously used to trace net evaporation rates in lakes (e.g., Gibson et al., 1993; Gat et al., 1994). The underlying mechanism is using the isotopic fractionation of oxygen and hydrogen atoms of the H_2O molecule in surface seawater during its evaporation. For thermohaline circulation, where seawater flow is driven by net evaporation it is possible to use the Rayleigh distillation equation (e.g. Craig et al., 1956; Appelo and Postma, 2005), given in section 2.2 below, to describe the isotopic composition of surface seawater while flowing and continuously loosing water by evaporation. The equation provides a simple relation between the fraction of remaining water molecules during evaporation and the isotopic changes in the ratio between the heavy (and rare) isotopes of ^{18}O and ^{2}H (deuterium, denoted by D) and the light (and abundant) isotopes ^{16}O and ^{1}H.

Here we derive a non-dimensional parameter which can estimate the "strength" of the thermohaline circulation. We use three independent methods to validate this parameter: salinity based measurements and isotopic measurements of $\delta^{18}O$ and δD in surface waters. We are interested in areas where excess of evaporation over precipitation dominates, in long term time scales of multi year average, neglecting seasonal variability, and thus we looked for

Ocean Sci. Discuss., https://doi.org/10.5194/os-2017-58
Manuscript under review for journal Ocean Sci.
Discussion started: 28 July 2017

areas of small horizontal velocities where the data is available to us. We found two areas suitable for the case study, one in a semi-enclosed basin (The Red Sea) and the second in the southwest Indian Ocean. The agreement of the independent methods will be an indirect confirmation of the validity of the estimates of thermohaline circulation strength. The method employs data collected from the Red Sea and the Gulf of Elat (Aqaba), and for the southwest Indian Ocean, but can be used for any thermohaline driven water mass where the flow in the surface layer is weak and driven by net evaporation.

2. Theory: Explicit expressions for the net evaporation

In this section we derive a single-parameter that quantifies the strength of the thermohaline circulation from changes of seawater salinity (subsection 2.1) and isotopic composition of $\delta^{18}O$ and/or δD (subsection 2.2).

2.1. Conservation of salt

The simple scenario we envision, involves seawater inflowing for year(s) subject to excess evaporation over precipitation at a rate of Q $m^3 \cdot y^{-1}$ (e.g. when water flows from an ocean into a semi-enclosed adjacent basin). Typical rates of evaporation worldwide are of order 1 meter per year ($\cong 3.17 \cdot 10^{-8}$ $m \cdot s^{-1}$). A simple mass balance of water and salt in the basin (assuming that density changes due to changes in salinity are second-order and can be neglected and that salinity is conserved in the mixed layer) leads to the following relation between salinity changes as a function of distance (similar to the classical Knudsen relation, formulated nearly 100 years ago (see Defant, 1961)):

$$S(x) \cdot \left(1 - \frac{Q}{V_0} \cdot t\right) = S(0) \qquad (1)$$

Ocean Sci. Discuss., https://doi.org/10.5194/os-2017-58
Manuscript under review for journal Ocean Sci.
Discussion started: 28 July 2017

where S is the salinity of the mixed layer [in dimensionless units], x [km] is the distance from the starting point of the water trajectory (i.e., x=0 denotes Bab el Mandeb in the case of the Red Sea), Q is the excess evaporation over precipitation [$m^3 \cdot d^{-1}$], V_0 is the volume of the mixed layer at the origin [m^3], $t = \frac{x}{u}$ is the time [d] that takes an arbitrary water volume to pass from x=0 to x [km] as it moves with the average speed u [$m \cdot d^{-1}$].

Substituting $Q = q \cdot A$ where q is the net evaporation flux [$cm \cdot d^{-1}$] and A is the cross-section area [cm^2] and letting $h = \frac{V(0)}{A}$ be the depth of the mixed layer transforms Eq. (1) to:

$$\frac{S(x)}{S(0)} = \frac{1}{\left(1 - \frac{q}{h} \cdot \frac{x}{u}\right)} = \frac{1}{(1-\gamma)} \qquad (2)$$

where the non-dimensional parameter in Eq. (2), $\gamma \equiv \frac{q}{h}\frac{x}{u}$, which arises naturally, quantifies the changes in salinity of the inflowing water due to net evaporation as a function of the distance from the origin.

This parameter that combines several physical parameters associated with the thermohaline circulation can also be written as $\gamma \equiv \frac{t_{adv}}{t_{evp}}$ where $t_{adv}=x/u$, is the advection time (i.e. time it takes a water parcel with velocity u to propagate the distance x) and $t_{evp}=q/h$, is the evaporation time (the time it takes to completely evaporate the mixed layer).

An examination of the characteristic magnitudes of the dimensional parameters in the Red Sea can provide an estimate for the non-dimensional model parameter γ. For x = 2000 km ($\cong 2 \cdot 10^6$ m) (the length of the Red Sea) and u = 1 $cm \cdot s^{-1}$ ($\cong 10^{-2}$ $m \cdot s^{-1}$) (annually averaged surface northward velocity along the sea; see figure 9 of Sofianos and Johns, 2003), assuming a mixed layer depth (annually averaged) of h = 100 m (see figure 13 of Sofianos and Johns, 2003) and a net evaporation of q = 2 $m \cdot y^{-1}$ ($\cong 6 \cdot 10^{-8}$ $m \cdot s^{-1}$) (see Sec. 1) the value of

Ocean Sci. Discuss., https://doi.org/10.5194/os-2017-58
Manuscript under review for journal Ocean Sci.
Discussion started: 28 July 2017

129 $\gamma \equiv \frac{q}{h}\frac{x}{u} \cong 0.1$. This value is small enough to justify a Taylor series expansion of the Right

130 Hand Side (RHS, hereafter) of Eq. (2) for γ<<1, namely $1/(1-\gamma) \cong 1+\gamma$. Rearranging the

131 terms that result from this expansion of the RHS of Eq. (2) yields the following simple

132 expression:

133 $$\frac{S(x)-S(0)}{S(0)} \cong \gamma \quad (3)$$

134 Eq. (3) describes the first order relationship between the relative changes in salinity and the

135 non-dimensional parameter γ.

136 For a linearly varying salinity $S(x)=a \cdot x+b$, (where a is the slope, b is the intercept and

137 x is the distance from the origin) the value of γ is estimated from Eq. (3) as:

138 $$\gamma = \frac{S(x)-S(0)}{S(0)} = \frac{(ax+b)-b}{b} = \frac{ax}{b} \quad (4)$$

139

140 2.2. Changes in isotopic composition

141 The oxygen isotopic composition of water undergoing evaporation during the travel within a

142 semi enclosed basin can be described using the Rayleigh equation (e.g., Craig et al., 1956;

143 Appelo and Postma, 2005) as follows:

144 $$\delta^{18}O_{water}(x) = \delta^{18}O_{water}(0) + \varepsilon_{v,w} \ln(f) \quad (5)$$

145 where $\delta^{18}O_{water}$ *(x)* and $\delta^{18}O_{water}$ *(x)* are the oxygen isotopic composition of the seawater [‰]

146 at distance x and at the origin respectively, expressed in δ notation, such that

147 $\delta^{18}O_{samle} = \frac{R_{sample} - R_{standerd}}{R_{sample}} \cdot 1000$, where R_{sample} and $R_{standard}$ are the isotopic ratios (rare to

148 abundant isotope) of the sample and the standard respectively; f is the fraction of liquid water

149 remaining after evaporation; $\varepsilon_{v,w} = 1000 \cdot (\alpha_{v,w} - 1)$ is the enrichment factor [‰] and

Ocean Sci. Discuss., https://doi.org/10.5194/os-2017-58
Manuscript under review for journal Ocean Sci.
Discussion started: 28 July 2017

150 $\alpha_{v,w} = \frac{R_{vapor}}{R_{water}}$ is the isotope fractionation factor between vapor and water, where R_{vapor} and

151 R_{water} are the isotopic ratios of the vapor and water, respectively.

152 Using the Rayleigh equation, Eq. (5), a relationship between the hydrogen and oxygen

153 isotopic composition of water and the thermohaline circulation can be derived. Values for α

154 were computed using the data of Majoube (1971) (see also Rohling, 2007) with a temperature

155 of 28°C, which yields $\alpha_{\delta^{18}O} = 0.9909$ or $\varepsilon_{v,w}$ = -9.1 ‰. Using the definition of *f*:

156 $$f = \frac{H_2{}^{16}O(x)}{H_2{}^{16}O(0)} = \frac{C_{H_2{}^{16}O(0)}V(x)}{C_{H_2{}^{16}O(0)}V(0)} = \frac{V(0)-Qt}{V(0)} = 1-\frac{q}{h}\frac{x}{u} = 1-\gamma \quad (6)$$

157 where $H_2{}^{16}O(x)$ and $H_2{}^{16}O(0)$ are the weight of light water molecules at *x* and at 0

158 respectively, $C_{H_2{}^{16}O(0)}$ is the concentration of light water molecules (g·cm^{-3}) and *V* is the

159 volume of water [cm^3]. Substituting Eq. (6) into Eq. (5) yields:

160 $$\frac{\delta^{18}O_{water}(x)-\delta^{18}O_{water}(0)}{\varepsilon_{v,w}} = \ln(1-\gamma) \quad (7)$$

161 For $(1-\gamma)\cong 1$, a Taylor expansion of $\ln(1-\gamma)$ near 1 yields the following relationship

162 between the non-dimensional parameter γ and the isotopic composition of oxygen:

163 $$\frac{\delta^{18}O_{water}(x)-\delta^{18}O_{water}(0)}{\varepsilon_{v,w}} = -\gamma \quad (8)$$

164 Similarly, one can derive the same relation for hydrogen isotopes by replacing in Eq.

165 (8) the variable $\delta^{18}O$ by δD and the corresponding enrichment factor for oxygen isotopes by

166 that of hydrogen isotopes, $\varepsilon_{v,w}$ = -70.9 ‰ as calculated from the fractionation factor for

167 hydrogen isotopes, $\alpha_{\delta D} = 0.9291$ (calculated from Majoube,1971, for temperature of 28°C).

168 For a linearly varying $\delta^{18}O$ (and similarly for δD) $\delta^{18}O(x)=a\cdot x+b$, (where *a* is the

169 slope, *b* is the intercept and *x* is the distance from the origin) the value of γ is estimated from

170 Eq. (8) as:

Ocean Sci. Discuss., https://doi.org/10.5194/os-2017-58
Manuscript under review for journal Ocean Sci.
Discussion started: 28 July 2017

171 $$\gamma = \frac{\delta^{18}O(0) - \delta^{18}O(x)}{\varepsilon} = \frac{b - (ax + b)}{\varepsilon} = \frac{-ax}{\varepsilon} \quad (9)$$

172 ## 3. Application to the Red Sea and South-West Indian Ocean

173 The salt conservation equation, Eq. (1) and the isotopic fractionation equation, Eq. (5) have
174 both yielded simple expressions that involve the same nondimensional parameter γ. In order
175 to apply these relationships to particular basins the advection time t_{adv} has to be large enough
176 to ensure that the relative changes in salinity and isotopic compositions are significant. In
177 order for this to hold, the ratio x/u has to be large i.e. the water moves slowly and/or the
178 propagation distance is large. Depending on the length of the trajectory and the speed of the
179 flowing water, t_{adv} can vary by orders of magnitude. In contrasts, the value of q varies by a
180 factor of 2 only in regions far from the tropics (where precipitation is high) and the poorly
181 heated Poles. Thus, q is of order 1 m/year ($\cong 3.15 \cdot 10^{-8}$ m·s^{-1}) in the subtropics and mid-
182 latitudes (see https://aquarius.umaine.edu/cgi/gal_images.htm?id=33) and since the depth of
183 the mixed layer h of order of tens of meters, $t_{evp}=h/q$ varies by a factor of 2-3 only. We have
184 identified two basins where the required data is freely accessible and where these constraints
185 on large t_{adv} and t_{evp} that exceeds 1 year are satisfied. These regions are analyzed next.
186
187 ### 3.1 Red Sea
188 #### 3.1.1. Hydrographic and Climatological Background
189 The circulation in the semi-enclosed Red Sea is strongly controlled by the net evaporation-
190 precipitation which is balanced by a net inflow through the straits of Bab el Mandeb that
191 connects the basin with the adjacent Indian Ocean. Though the currents associated with the
192 thermohaline circulation in semi-enclosed basins are fairly weak they provide the main
193 transport mechanism into the basin for heat, salt, nutrients and plankton. General reviews of
194 this important circulation with low-speed currents in semi-enclosed basins are given in

Ocean Sci. Discuss., https://doi.org/10.5194/os-2017-58
Manuscript under review for journal Ocean Sci.
Discussion started: 28 July 2017

195 Pickard and Emery (1990) and Spall (2003) and specifically for the Red Sea in Zhai et al.
196 (2015).

197 Under steady state conditions, the amount of net evaporation can be estimated from
198 the difference in the salinity between the inflowing and outflowing waters by the Knudsen
199 relation. The outflowing water from the high salinity Red Sea to the Indian Ocean maintains
200 the steady state in salinity and water mass/volume inside the Red Sea. The time scale for
201 surface water to propagate from the straits of Bab el Mandeb to the northern tip of the Gulf of
202 Elat (Aqaba) is about 6 years (for x=2000 km and u=1 cm/s the travel time is $\cong 1.9 \cdot 10^8$ s).

203 3.1.2. Data

204 The salinity and isotopic data used for the Red Sea were measured on seawater sampled
205 between October 23 and November 6, 1998 during cruises of R/V Sea Surveyor from the city
206 of Elat to the Seychelles archipelago (Fig. 1.a.; Steiner et al., 2014). Surface seawater samples
207 were collected underway every ~100 km using a specially designed water sampler (detailed
208 information on sampling, salinity and isotopic analyses and data acquisition in Steiner et al.,
209 2014).

Ocean Sci. Discuss., https://doi.org/10.5194/os-2017-58
Manuscript under review for journal Ocean Sci.
Discussion started: 28 July 2017

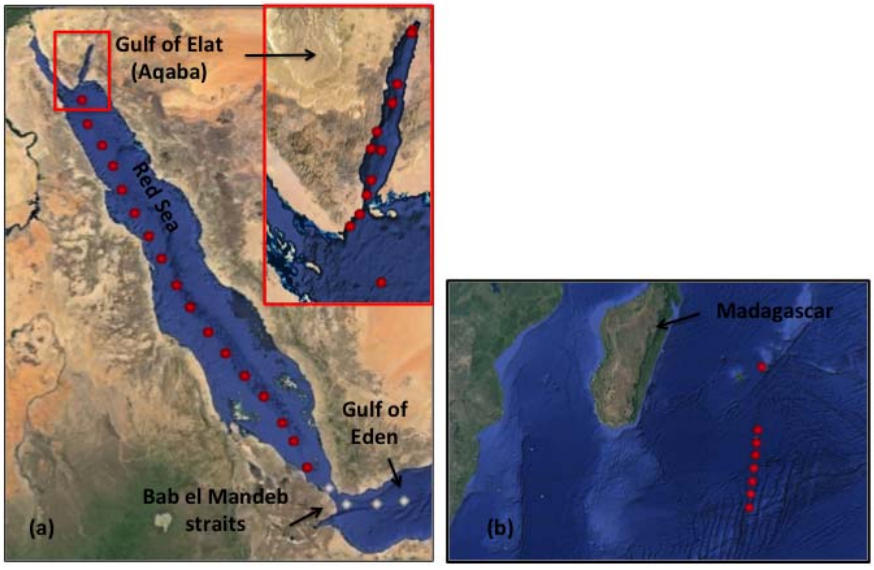

Figure 1: (a, left panel): Satellite image of the Red Sea with inset representing a zoom into the Gulf of Elat (Aqaba) (adopted from Steiner et al., 2014). Red points represent Red Sea sampling stations and white points represent Bab el Mandeb and Gulf of Aden stations (see text for explanation). Salinity, $\delta^{18}O$ and δD values for surface waters of Red Sea-Gulf of Aden were taken from Steiner et al., 2014. (b, right panel): Satellite image of the Southern Indian Ocean showing surface waters sampling stations (red dots). Salinity and $\delta^{18}O$ values were taken from Srivastava et al., 2007.

High Correlation between $\delta^{18}O$, δD and salinity has been previously reported in the Red Sea by Craig (1966) and Steiner et al. (2014). The value of the three variables, salinity, $\delta^{18}O$ and δD were each plotted against their distance from Bab el Mandeb (x) and linear regression lines were calculated to obtain intercepts and slopes for calculating the non-dimensional parameter γ (Fig. 2, Eq. (4) and Eq. (9), Table 1). The value of each variable at x=0 (y intercept) was constrained from the average of 4 measurements close to the Bab el Mandeb straits (white points in Fig. 1). Since the time scale of this flow is 6 years ($\cong 1.9 \cdot 10^8$ s) (Section 3.1.1.), the measurements during the 2-week cruise in which the entire 2,000 km of the length of the sea was sampled represent annually averaged values. Moreover, the similarity in the $\delta^{18}O$ and δD versus salinity plots for the years 1962 (Craig, 1966) and 1998

Ocean Sci. Discuss., https://doi.org/10.5194/os-2017-58
Manuscript under review for journal Ocean Sci.
Discussion started: 28 July 2017

(Steiner et al., 2014), a 36 years period, suggests that the cross-section of these parameters along the Red Sea represents a long-term steady state.

3.1.3. Results

Figure 2 shows the linear best fit of changes in salinity, $\delta^{18}O$ and δD with distance from Bab-el-Mandab. These best fitting lines have R^2= 0.89 for salinity, R^2 = 0.85 for $\delta^{18}O$ and R^2=0.76 for δD. The value of γ is calculated from the intercepts and slopes of the best fitting lines from Eq. (4) and Eq. (9) and the resulting estimates for γ are given in Table 1. The confidence intervals of these estimates were calculated from the uncertainty in the regression slopes. The values of the non-dimensional parameter, γ, calculated from the oxygen and hydrogen isotopic data agree very well with each other and both of these estimates fall within the 95% confidence interval of salinity (Table 1, third column) with an average value of 0.1.

Sensitivity of the calculated values to the enrichment factor (α) of $\delta^{18}O$ was tested by using two different methods: 1) testing sensitivity to the specific formula by which the enrichment factor is calculated using Dansgaard (1964; see section 1.2) instead of Majoube (1971); and 2) changing the mean temperature used to calculate the enrichment factor in both formulas (Majoube, 1971; Dansgaard, 1964) in the range of 28±1.5°C, the annual mean temperature of the Red Sea (Nandkeolyar et al., 2013). Both methods show that the values found for the non-dimensional parameter γ are robust and the uncertainty due to the variations in temperature or formulae used for the calculations results in variations that are smaller than the confidence interval given in Table 1.

Ocean Sci. Discuss., https://doi.org/10.5194/os-2017-58
Manuscript under review for journal Ocean Sci.
Discussion started: 28 July 2017

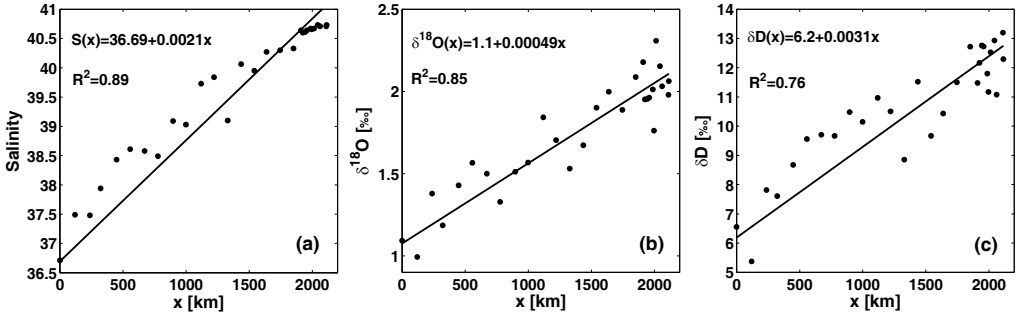

Figure 2: Salinity (a), $\delta^{18}O$ (b) and δD (c) as a function of the distance from the straits of Bab el Mandeb (x).

Table 1: Estimates of the non-dimensional parameter γ, based on salinity, $\delta^{18}O$ and δD. The values of this parameter in column 3 were calculated from the slopes and intercepts of the corresponding best-fit equations: Eq. (4) and Eq. (9) for salinity and $\delta^{18}O$, respectively and an equation similar to Eq. (9) but for δD instead of $\delta^{18}O$. x is the distance from the Bab el Mandeb straits.

Proxy variable	Best fit from data in Fig. 2	γ and 95% confidence interval
Sea Surface Salinity	$S(x)=36.69+0.0021x$	0.11±0.01
$\delta^{18}O$	$\delta^{18}O(x)=1.1+0.00049x$	0.12±0.02
δD	$\delta D(x)=6.2+0.0031x$	0.09±0.02

3.2 The South-West Indian Ocean

3.2.1. Hydrographic and Climatological background

The subtropical anti-cyclonic Indian Ocean gyre consists of two western boundary currents, the strong Agulhas current west of Madagascar and a weaker East Madagascar current. We have located a second suitable study area, where the necessary data is available, east of the East Madagascar Current where the water flows southward. This 20°S-30°S segment at ~57 °E is located on the border between the tropics and subtropics (Figure 1). In contrast to the semi enclosed Red Sea, where data has been collected for many years, the selected segment in the South-West Indian Ocean is a small part of the subtropical gyre, and the details of the hydrographic conditions along it are not known with sufficient accuracy (Stramma and

Ocean Sci. Discuss., https://doi.org/10.5194/os-2017-58
Manuscript under review for journal Ocean Sci.
Discussion started: 28 July 2017

Lutjeharms, 1997). As a result, the annual velocities, mixed layer depth and evaporation rate are less certain in this segment compared with those of the Red Sea. Since this is not a western boundary current we assume that the mean velocities here are sufficiently small (no more than a few centimeters per second) so that the advection time scale along this 1000 km long segment is more than 1 year. Since along this segment evaporation exceeds precipitation and the advection time is of the order of at least 1 year we treat this segment as suitable for our analyses. The variation in isotopic composition and salinity along this segment is rather small because the area north to latitude 20°S is relatively close to the Tropics and hence excess evaporation is rather small (see e.g. https://aquarius.umaine.edu/cgi/gal_images.htm?id=33) and the direction of flow is not consistently southward.

3.2.2. Data

Salinity and $\delta^{18}O$ data reported in Srivastava et al., 2007 were downloaded from the World Ocean Atlas (https://www.nodc.noaa.gov) for the region between 20°S-30°S and at ~57 °E (Fig. 1b). Similar to the Red Sea, high correlation between $\delta^{18}O$ was reported along this segment by Srivastava et al. (2007), who suggested that the changes in isotopic ratio are related with the excess of evaporation over precipitation along this segment. These specific latitudes were chosen since they lie south of the Tropics (where precipitation exceeds evaporation) and north of the North Sub-Tropical Front (south of which lie the Sub-Tropical Mode Water) (see details in figure 1 of Srivastava et al., 2007).

3.2.3. Results

Figure 3 shows the linear best fit of changes in $\delta^{18}O$ and salinity along the segment: the quality of the best fitting lines is given R^2= 0.91 for $\delta^{18}O$ and R^2 = 0.87 for salinity. Table 2 summarizes the corresponding values of γ in the two calculations and the confidence intervals

Ocean Sci. Discuss., https://doi.org/10.5194/os-2017-58
Manuscript under review for journal Ocean Sci.
Discussion started: 28 July 2017

of the estimates from the two variables barely overlap giving an average γ value of 0.02 about 5 fold smaller than the γ of the Red Sea.

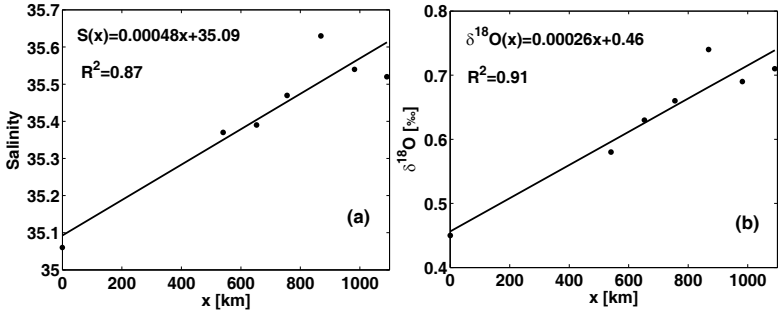

Figure 3: Salinity (a) and $\delta^{18}O$ (b) as a function of the distance from the most northern point in 5°N.

Table 2: Estimates of the non-dimensional parameter γ based on salinity and $\delta^{18}O$ in the Indian Ocean. The values of this parameter in column 3 were calculated from the slopes and intercepts of the corresponding best-fit equations: Eq. (4) and Eq. (9) for salinity and $\delta^{18}O$. x is the distance southward of 20°S.

Proxy variable	Best fit from data in Fig. 2	γ and 95% confidence interval
Sea Surface Salinity	$S(x)=35.09+0.00048x$	0.01±0.01
$\delta^{18}O$	$\delta^{18}O(x)=0.46+0.00026x$	0.03±0.01

4. Discussion

In this paper we derive, for the first time, a non-dimensional parameter γ that estimates the "strength" of the thermohaline circulation. The parameter γ arises naturally from the equations that express the conservation of such quantities as salt or certain isotopes that change in response to intense evaporation. The non-dimensional parameter γ combines four dimensional parameters that govern the thermohaline circulation: the velocity of the flow (u); the depth of the mixed layer (h); the length of water trajectory (x); and the evaporation rate along the trajectory (q). Thus, when γ is known any 3 of these dimensional parameters provides an

Ocean Sci. Discuss., https://doi.org/10.5194/os-2017-58
Manuscript under review for journal Ocean Sci.
Discussion started: 28 July 2017

estimate of the fourth. It was shown in section 2.1 that γ is the t_{adv}/t_{evp} ratio, which are the time to pass a typical distance by advection (t_{adv}) and the time to completely evaporate the mixed layer (t_{evp}).

By the use of data collected from two different areas (from hydrological viewpoint) – the Red Sea and the South-West Indian Ocean – we find that the resulting values of γ from three independent variables of: salinity, $\delta^{18}O$ and δD are nearly identical. By the use of typical scales for the Red Sea (for x=2000 km, h=100 m and u=1 cm·s^{-1}), our estimation of the excess evaporation, q, are 1.8±0.2 m·y^{-1} for salinity variations, 1.7±0.3 m·y^{-1} from $\delta^{18}O$ variations and 1.4±0.2 m·y^{-1} from δD variations. Despite the simplicity of this model and neglecting other important physical processes, these estimates are in excellent agreement with previously calculated estimates in the same region of 1.6-1.8 m·y^{-1} (e.g., Tragou, 1999; Ben-Sasson et al., 1999). Comparing the estimates that result from the various variables leads to the conclusion that the simpler indirect methods yield consistent estimates that differ only slightly from the elaborate direct method of detailed heat budget balance. Similarly, although the parameters in the Indian are less certain than in the Red Sea, for x=1000 km, h=100 m and q=1 m·y^{-1} the estimate for the advection velocity is of order 1-3 cm·s^{-1} i.e. an advection time of order 1 year.

The isotopic data complements the salinity data and can be used either for validating estimates based on salinity changes or to substitute them. Though the accuracy of *in-situ* salinity measurement is higher than that of isotopic ratios our results (Figs. 2, 3) suggest that both variables yield similarly correlated cross-sections that are equally appropriate for deriving reliable estimates of γ in diverse oceanographic settings. However, from a practical viewpoint and given present day technology it is much easier to measure salinity than isotopic ratios. When one recalls the tremendous improvement that took place in the last decades in the ease (and accuracy) of measuring salinity it is not unreasonable to expect that in the coming decades similar improvement will take place in the ease (and accuracy) of measuring

Ocean Sci. Discuss., https://doi.org/10.5194/os-2017-58
Manuscript under review for journal Ocean Sci.
Discussion started: 28 July 2017

isotopic ratios. At that time it will be possible to use our method routinely for verifying salinity-based estimates of net evaporation.

To appreciate the physical meaning of the non-dimensional parameter γ we envision the following two extreme scenarios, or asymptotes of γ. First consider the case of very small γ, i.e. when advection is very strong such as the western boundary currents where salinity differences along the trajectory are too small (i.e. the water propagates too fast for the salinity signal to be meaningful). In this case, t_{adv} is in the order of days, (for u=1 m·s^{-1} and x=1000 km), while t_{evp} is of order 100 years in the most extreme case (q=1 m·y^{-1} and h=100m) so the corresponding value of γ is ~10^{-5}. In this scenario, water flow is not controlled by excess evaporation. The second scenario is that of γ=1 where the evaporation time equals the advection time, i.e. when all the water in the mixed layer is evaporated while flowing over the typical distance x. In this scenario, the evaporation and advection along the trajectory are highly correlated and the (thermohaline) flow is driven by the excess evaporation.

As in other non-dimensional parameters, γ has a physical meaning that can be appreciated by examining the ratio between the advection and evaporation times. The approach we advocate is similar to that employed in deciphering the physical meaning of the Rossby number, that quantifies the deviation of the flow from geostrophic balance (the smaller the Rossby number is, the closer the flow is to geostrophic balance). The parameter $\gamma << 1$ is viewed as a measure of the degree to which the flow is thermohaline: When γ is tiny (~10^{-5}) the flow is far from thermohaline as in Western Boundary currents while when $\gamma \leq 1$ the flow is close to being purely thermohaline as in the Red Sea and the Indian Ocean. The difference of about 5-fold between the values of γ in the two ocean regions (see Tables 1 and 2) suggest that the flow in Red Sea is closer to being thermohaline more than the flow in Indian Ocean, i.e., that the thermohaline flow in the former is driven by evaporation more than that in the latter. However, this interpretation is not conclusive and may be result from a combination of

the slightly different values of x and h in the two sites in addition to differences in the values of u, q. If all four physical parameters in $\gamma<1$ are known (e.g. when a numerical model provides their typical values) in a certain basin its value can be easily calculated to provide a measure of the degree to which the circulation there is thermohaline. The usefulness of γ will be determined by the degree to which the scientific community finds it helpful in interpreting oceanic observations.

ACKNOWLEDGMENTS

The authors wish to thank the director and staff of the Inter University Institute for Marine Sciences in Eilat for organizing the cruise of RV Sea Surveyor during which which the Red Sea data were collected. We acknowledge the Israel Science Foundation for continued support that enabled obtaining the Red Sea data for this research.

References

Appelo, C. A. J., Postma, D.: Geochemistry, groundwater and pollution. CRC press. Chapter 2, pages 33-37, 2005.

Assaf, G. and Kessler, J.: Climate and energy exchange in the Gulf of Aqaba (Eilat). Monthly Weather Review, 104(4), pp.381-385, doi: 10.1175/1520-0493(1976)104<0381:CAEEIT>2.0.CO;2, 1976.

Ben-Sasson, M., Brenner, S., Paldor, N.: Estimating air-sea heat fluxes in semi-enclosed basins: The case of the Gulf of Elat (Aqaba). Journal of Physical Oceanography 39 (1), 185–202, doi: 10.1175/2008JPO3858.1, 2009.

Berman, T., Paldor, N. and Brenner, S.: Annual SST cycle in the Eastern Mediterranean, Red Sea and Gulf of Elat. Geophys. Res. Lett., 30(5), 1261. doi:10.1029/2002GL015860, 2003.

388 Bogdanova, A.K.: Indirect estimation of the seasonal variation of the water exchange through
389 Bab el Mandeb. L'oceanographie physique de la Mer Rouge, CNEXO, Paris, pp.253-
390 265, 1974.
391 Cohen, Y., Krumbein, W. E., Goldberg, M., Shilo, M.: Solar lake (Sinai). 1. Physical and
392 chemical limnology. Limnology and Oceanography 22 (4), 597–608, doi:
393 10.4319/lo.1977.22.4.0597, 1974.
394 Craig, H., Boato, G., White, D. E.: Isotopic geochemistry of thermal waters. In: Proc. 2nd
395 Conf. on Nuclear Processes in Geologic Settings. Vol. 19. National Academy of
396 Science, National Research Council, pp. 19–44, 1956.
397 Craig H.: Isotopic composition and origin of the Red Sea and Salton Sea geothermal
398 brines. Science 154(3756):1544–1548, doi: 10.1126/science.154.3756.1544, 1966.
399 Dansgaard, W.: Stable isotopes in precipitation. Tellus A 16 (4), 1964.
400 Defant, A.: Physical oceanography; Pergamon Press, Volume 2, Chapter 12 pages: 379-381,
401 1961.
402 Gat, J. R., Bowser, C. J., Kendall, C.: The contribution of evaporation from the great lakes to
403 the continental atmosphere: estimate based on stable isotope data. Geophysical
404 Research Letters 21 (7), 557–560, doi: 10.1029/94GL00069, 1994.
405 Gibson, J., Edwards, T., Bursey, G., Prowse, T.: Estimating evaporation using stable isotopes:
406 quantitative results and sensitivity analysis for two catchments in northern Canada.
407 Nordic Hydrology 24, 79–94, 1993.
408 Majoube, M.: Fractionnement en oxygene-18 et en deuterium entre leau et sa vapeur. J. Chim.
409 phys 68 (7-8), 1423–1436, doi: 10.1051/jcp/1971681423, 1971.
410 Nandkeolyar, N., Raman, M., Kiran, G.S.: Comparative analysis of sea surface temperature
411 pattern in the eastern and western gulfs of Arabian Sea and the Red Sea in recent past

using satellite data. International Journal of Oceanography, doi: 10.1155/2013/501602, 2013.

Pickard, G.L. and Emery, W.J.: Descriptive physical oceanography: an introduction. Elsevier, 1990.

Rohling, E.J.: Oxygen isotope composition of seawater. Encyclopedia of quaternary science, 3, pp.1748-1756, 2007.

Sofianos, S., Johns, W., Murray, S.: Heat and freshwater budgets in the Red Sea from direct observations at Bab el Mandeb. Deep Sea Research Part II: Topical Studies in Oceanography 49 (7), 1323–1340, doi: 10.1016/S0967-0645(01)00164-3, 2002.

Sofianos, S. S., & Johns, W. E.: An oceanic general circulation model (OGCM) investigation of the Red Sea circulation: 2. Three-dimensional circulation in the Red Sea. Journal of Geophysical Research: Oceans, 108(C3), doi: 10.1029/2001JC001185, 2003.

Spall, M.A.: On the thermohaline circulation in flat bottom marginal seas. Journal of Marine Research, 61(1), pp.1-25, doi: 10.1357/002224003321586390, 2003.

Srivastava, R., Ramesh, R., Prakash, S., Anilkumar, N. and Sudhakar, M.: Oxygen isotope and salinity variations in the Indian sector of the Southern Ocean. Geophysical Research Letters, 34(24), doi: 10.1029/2007GL031790, 2007.

Steiner, Z., Erez, J., Shemesh, A., Yam, R., Katz, A., Lazar, B.: Basin-scale estimates of pelagic and coral reef calcification in the Red Sea and western Indian Ocean. Proceedings of the National Academy of Sciences 111 (46), 16303–16308, doi: 10.1073/pnas.1414323111, 2014.

Stramma, L. and Lutjeharms, J.R.: The flow field of the subtropical gyre of the South Indian Ocean. Journal of Geophysical Research: Oceans, 102(C3), pp.5513-5530, 10.1029/96JC03455, 1997.

436 Tragou, E., Garrett, C., Outerbridge, R., Gilman, C.: The heat and freshwater budgets of the
437 Red Sea. Journal of physical oceanography 29 (10), 2504–2522, doi: 10.1175/1520-
438 0485(1999)029<2504:THAFBO>2.0.CO;2, 1999.
439 Vercelli, F.: Bilancio dello scambio di acque fra mar roseo r.n. Ricerche di oceanografia fisica
440 12, 178–183, 1925.
441 Zhai, P., Pratt, L.J. and Bower, A.: On the crossover of boundary currents in an idealized
442 model of the Red Sea. Journal of Physical Oceanography, 45(5), pp.1410-1425, doi:
443 10.1175/JPO-D-14-0192.1, 2015.